
Article:
Drummond, R. orcid.org/0000-0002-2586-1718, Zhao, S., Howey, D.A. et al. (1 more author) (2017) Circuit synthesis of electrochemical supercapacitor models. Journal of Energy Storage, 10. pp. 48-55. ISSN 2352-152X

https://doi.org/10.1016/j.est.2016.11.003

Circuit Synthesis of Electrochemical Supercapacitor Models

R. Drummond, S. Zhao, D.A. Howey and S. R. Duncan

***Abstract*—This paper considers the synthesis of RC electrical circuits from physics-based supercapacitor models that describe conservation and diffusion relationships. The proposed synthesis procedure uses model discretisation, linearisation, balanced model order reduction and passive network synthesis to form the circuits. Circuits with different topologies are synthesized from physical models. Because the synthesized impedance functions are generated by considering the physics, rather than from experimental fitting which may ignore dynamics, this work provides greater understanding of the physical interpretation of electrical circuits and will enable the development of more generalised circuits.**

***Index Terms*—Supercapacitors, Electrochemical Modelling, Equivalent Circuits, Passive Network Synthesis**

I. Introduction

Electric double layer (EDL) supercapacitors, otherwise known as supercapacitors or ultracapacitors, are an increasingly popular form of energy storage device, which are characterised by high power densities, long lifespans, low temperature dependencies and low internal resistances [1]. The main energy storage mechanism of EDL supercapacitors does not involve chemical reactions, but instead uses charge separation across the double layer in porous electrodes with high specific surface areas [2]. This results in supercapacitors typically having lower energy densities, but higher power densities than devices such as lithium ion batteries, which utilise chemical energy storage, and increased energy densities compared to dielectric capacitors [3]. Supercapacitors are typically used for high power applications, for example, in delivering the transient loads when connected in a hybrid power system with lithium ion batteries [4]. In a hybrid power system, the benefits of the different devices can be combined to give improved performance and reduced battery degradation, since the battery can then be operated at near steady-state conditions.

The growing popularity of supercapacitors has led to a demand for improved performance and understanding from a systems perspective. An important tool to achieve this improved performance is the development of models that enable predictions to be made about the supercapacitor during a charge, reducing experiment numbers and enabling a constructive methodology for design. The literature on supercapacitor modelling is both large and growing, with the models being mainly differentiated by their accuracy, complexity and detail. The two main categories of supercapacitor models are equivalent circuits (EC) and physics based (PB) models. EC models are formed by the connection of passive circuit components such as resistors and capacitors [5]. For supercapacitors, the resulting model equations are typically low-order linear ordinary differential equations (ODEs) which are relatively straight forward to solve. This makes EC models both simple to implement and to understand, resulting in them being the most popular form of model for application purposes. The main drawback of EC models is that the model states have little physical interpretation and the developed circuits are typically local approximations of the nonlinear devices. This limits their use for design purposes and for gaining a detailed understanding about the physical state of the device during a charge. Numerous EC models have been presented in the literature [6, 7, 8], with three common circuits being compared in [9] for an electric vehicle application.

PB models are formed from a set of partial differential equations (PDEs) that describe the electrochemistry of the device. These PDEs typically describe diffusion equations coupled with algebraic constraints to enforce charge conservation [10]. Since the underlying equations are PDEs, PB models are generally more complex than EC models and are usually implemented with some form of spatial discretisation technique, such as the finite difference method [10]. In [10], the physical PDE equations were established and shown to match experimental data reasonably well. Several studies have expanded upon this PB model, for example, by studying electrode 3D effects and parameter sensitivities [11], the computational implementation with an efficient spectral collocation discretisation [12], implementation with the multi-physics modelling programme COMSOL [13], a reduced order PDE system where concentration effects were ignored [14], the inclusion of temperature effects [15] and analytic solutions for constant current and electrical impedance spectroscopy charging profiles are given in [16]. Physics based models have also been developed for related electrical energy storage devices. For example, the Newman model [17] has been widely studied for lithium-ion batteries, both in terms of its implementation [18] and its incorporation within a control

R. Drummond, S. Zhao, D.A. Howey and S. R. Duncan are with the Department of Engineering Science, University of Oxford, 17 Parks Road, OX1 3PJ Oxford, United Kingdom, Email: {ross.drummond,shi.zhao,david.howey,stephen.duncan}@eng.ox.ac.uk.
Work supported by the Engineering and Physical Sciences Research Council project J010537/1.

system [19].

Even though both EC and PB supercapacitor models describe the same physical device, there has not been much overlap between the two methods and they are often treated as two separate approaches. Those efforts that have been made to link the approaches tend to give a qualitative, rather than quantitative, relationship between the two. The purpose of this paper is to bridge this gap by linking the two approaches using a mathematical transformation, such that equivalent circuits can be synthesized from the physical PDEs. This mathematical transformation uses balanced model order reduction [20] and passive network synthesis [21]. In order for circuits to be realised, it is necessary to give a state-space realisation of the impedance function. State-space realisations of analytic impedance functions using model order reduction and Taylor series expansion for PB lithium ion models was studied by Smith et al in [22, 23] and this paper is concerned with the circuit synthesis of similar realisations. The work of this paper could be said to generalise [24], where a specific circuit is designed to describe a PB lithium ion model, since the goal of this paper is show that a wide *class* of PB models can be synthesised into a wide *class* of circuits. The circuits developed by this approach have a physical basis and should be more robust than those which fit an impedance function to data.

It is stressed that the presented method does not give analytic expressions for the various components of the synthesized circuits in terms of the physical parameters of the device. Instead, a numerical procedure is introduced that allows the circuit synthesize to be efficiently carried out. The reason no analytic expression can be obtained is due to the model order reduction which results in a loss of model information. It should be noted that this work does not focus on model *development*, but instead on PB model *analysis* in terms of electrical components. For this reason, the models considered in this paper are not validated against experimental data, but, this validation was considered in [10, 25] amongst others.

The paper is structured as follows; PB and EC supercapacitor models are respectively described in Sections 2 and 3. Section 4 describes the synthesis process that uses passive network synthesis and model order reduction to form circuits from the PB model.

II. Physics Based Models

A particular PB supercapacitor model will now be described for the purpose of circuit synthesis but it is noted that the synthesis process of Section 4 is flexible enough to be applied on other PB models described by different physical equations. This PB model was developed in [12] and is a reformulation of the model set out in [10]. For the purposes of this paper, this PB model is treated as a 'true' model which describes the whole dynamics of the device and was shown to match up with experimental data [10, 25]. The model has three domains, one for each electrode and one for the separator, with the electrically insulating separator preventing a short circuit. In order

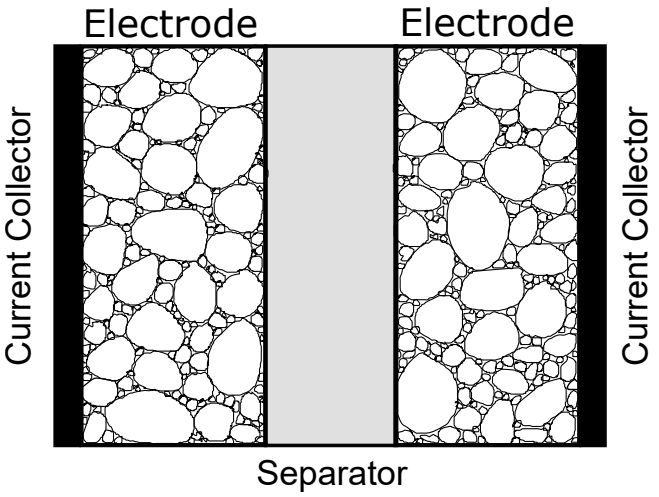

Figure 1: The standard construction of a supercapacitor.

for the model to be tractable, several assumptions have to be introduced, as outlined in [10]. These include the homogenisation of the electrode structure using porous electrode theory and fixing the capacitance as a lumped parameter, even though capacitance has been shown to change with variables such as the voltage [26]. The boundary conditions of the model are also outlined in [10] and are applied at the separator/electrode and current collector/electrode interfaces. These boundary conditions can be summarised as enforcing conservation of ionic flux and current. The current collectors are responsible for the transfer of current to and from the system. This setup is shown in Fig. 1.

The three partial differential algebraic equations of the PB model describe:

- Charge conservation across the double layer

$$aC\frac{\partial(\phi_1-\phi_2)}{\partial t}=\sigma\frac{\partial^2\phi_1}{\partial\chi^2} \tag{1a}$$

- Elctrolyte diffusion

$$\epsilon\frac{\partial c}{\partial t}=D\frac{\partial^2 c}{\partial\chi^2}-\frac{aC}{F}\left(t_-\frac{dq_+}{dq}+t_+\frac{dq_-}{dq}\right)\frac{\partial(\phi_1-\phi_2)}{\partial t}, \tag{1b}$$

- Ohm's Law

$$\kappa\left(\frac{RT(t_+-t_-)}{F}\right)\frac{\partial}{\partial\chi}\ln(c)+\sigma\frac{\partial(\phi_1-\phi_2)}{\partial\chi} + \left(\kappa\frac{\partial}{\partial\chi}+\sigma\frac{\partial}{\partial\chi}\right)\phi_2+i=0 \tag{1c}$$

with specific capacitance aC, potential in the electrode ϕ_1, potential in the electrolyte ϕ_2, electrode conductivity σ, porosity ϵ, diffusion constant D, Faraday constant F, transference numbers t_+ and t_-, $\frac{dq_{+/-}}{dq}$ describing the change in surface concentration of an ion associated with a change in the surface charge on the electrode q, electrolyte conductivity κ, gas constant R, temperature T, current density i and spatial co-ordinate χ. The values of these parameters used in this model based on a SAFT America

$$\begin{bmatrix} \epsilon & \frac{aC}{F}(t_- \frac{dq_+}{dq} + t_+ \frac{dq_-}{dq}) & 0 \\ 0 & aC & 0 \\ 0 & 0 & 0 \end{bmatrix} \begin{bmatrix} \dot{c} \\ \dot{\phi}_1 - \dot{\phi}_2 \\ \dot{\phi}_2 \end{bmatrix} = \begin{bmatrix} D\frac{\partial^2}{\partial \chi^2} & 0 & 0 \\ 0 & \sigma \frac{\partial^2}{\partial \chi^2} & \sigma \frac{\partial^2}{\partial \chi^2} \\ 0 & \sigma \frac{\partial}{\partial \chi} & \kappa \frac{\partial}{\partial \chi} + \sigma \frac{\partial}{\partial \chi} \end{bmatrix} \begin{bmatrix} c \\ \phi_1 - \phi_2 \\ \phi_2 \end{bmatrix} + \begin{bmatrix} 0 \\ 0 \\ \frac{\kappa RT(t_+ - t_-)}{F} \frac{\partial}{\partial \chi} \end{bmatrix} \ln(c) + \begin{bmatrix} 0 \\ 0 \\ 1 \end{bmatrix} i \tag{3a}$$

$$\begin{bmatrix} \epsilon & 0 \\ 0 & 0 \end{bmatrix} \begin{bmatrix} \dot{c} \\ \dot{\phi}_2 \end{bmatrix} = \begin{bmatrix} D\frac{\partial^2}{\partial \chi^2} & 0 \\ 0 & \kappa \frac{\partial}{\partial \chi} \end{bmatrix} \begin{bmatrix} c \\ \phi_2 \end{bmatrix} + \begin{bmatrix} 0 \\ \kappa\left(\frac{t_+ - t_-}{f}\right) \frac{\partial}{\partial \chi} \end{bmatrix} \ln(c) + \begin{bmatrix} 0 \\ 1 \end{bmatrix} i. \tag{3b}$$

supercapacitor are given in Table I. The output of the model y is the voltage V

$$y = V = \phi_1|_{x=0} - \phi_1|_{x=L}. \tag{2}$$

In the electrodes, equations (1a), (1b) and (1c) have state-space form (3a) and the state space form of the separator is given by (3b).

In implementation, discretisation methods are applied to the spatial differentiation operators of partial differential algebraic equations (DAE) systems such as (3a). Discretisation gives a finite dimensional approximation to the infinite dimensional PDE problem, resulting in a significantly simpler problem to solve. Upon discretisation, the spatial derivative operator $\partial/\partial\chi$ is approximated by a differentiation matrix $\hat{\mathbf{D}}_\zeta$, with the subscript ζ implying that the matrix accounts for ζ's boundary conditions. These boundary conditions are enforced by the patching technique of [27]. As outlined in [12], the spectral collocation method is used to discretise the model equations as this results in lower order models for a given level of solution accuracy [27]. The discretised version of the electrode state-space system (3a) is

$$\begin{aligned} &\begin{bmatrix} \epsilon & \frac{aC}{F}(t_- \frac{dq_+}{dq} + t_+ \frac{dq_-}{dq}) & 0 \\ 0 & aC & 0 \\ 0 & 0 & 0 \end{bmatrix} \begin{bmatrix} \dot{\mathbf{c}} \\ \dot{\phi}_{\mathbf{1}} - \dot{\phi}_{\mathbf{2}} \\ \dot{\phi}_{\mathbf{2}} \end{bmatrix} = \\ &\qquad \begin{bmatrix} D\hat{\mathbf{D}}_c^2 & 0 & 0 \\ 0 & \sigma\hat{\mathbf{D}}_{\phi_1}^2 & \sigma\hat{\mathbf{D}}_{\phi_1}^2 \\ 0 & \sigma\hat{\mathbf{D}}_{\phi_1} & \kappa\hat{\mathbf{D}}_{\phi_2} + \sigma\hat{\mathbf{D}}_{\phi_1} \end{bmatrix} \begin{bmatrix} \mathbf{c} \\ \phi_{\mathbf{1}} - \phi_{\mathbf{2}} \\ \phi_{\mathbf{2}} \end{bmatrix} \\ &\quad + \begin{bmatrix} 0 \\ 0 \\ \kappa\left(\frac{RT(t_+ - t_-)}{F}\right)\hat{\mathbf{D}}_{\ln c} \end{bmatrix} \ln(\mathbf{c}) + \begin{bmatrix} 0 \\ 0 \\ 1 \end{bmatrix} i, \end{aligned} \tag{4}$$

and, similarly, for the separator

$$\begin{aligned} \begin{bmatrix} \epsilon & 0 \\ 0 & 0 \end{bmatrix} \begin{bmatrix} \dot{\mathbf{c}} \\ \dot{\phi}_{\mathbf{2}} \end{bmatrix} &= \begin{bmatrix} D\hat{\mathbf{D}}_c^2 & 0 \\ 0 & \kappa\hat{\mathbf{D}}_{\phi_2}^2 \end{bmatrix} \begin{bmatrix} \mathbf{c} \\ \phi_{\mathbf{2}} \end{bmatrix} \\ &\quad + \begin{bmatrix} 0 \\ \kappa\left(\frac{RT(t_+ - t_-)}{F}\right)\hat{\mathbf{D}}_{\ln c} \end{bmatrix} \ln(\mathbf{c}) + \begin{bmatrix} 0 \\ 1 \end{bmatrix} i. \end{aligned} \tag{5}$$

In the following analysis, only (4) will be studied as (5) can be embedded into the structure of (4) by expanding the dimension of the model states. The discretised version of the model output is

$$y = \begin{bmatrix} 0 & C_1 \end{bmatrix} \begin{bmatrix} \mathbf{c} \\ \phi_{\mathbf{1}} - \phi_{\mathbf{2}} \end{bmatrix} + C_1\phi_{\mathbf{2}} + D_1 i. \tag{6}$$

It is possible to convert the DAE (4) into an ODE by solving the algebraic equation

$$\sigma\hat{\mathbf{D}}_{\phi_1}(\phi_{\mathbf{1}} - \phi_{\mathbf{2}}) + \left(\kappa\hat{\mathbf{D}}_{\phi_2} + \sigma\hat{\mathbf{D}}_{\phi_1}\right)\phi_{\mathbf{2}} \tag{7}$$

$$\kappa\left(\frac{t_+ - t_-}{f}\right)\hat{\mathbf{D}}_{\ln c}\ln(\mathbf{c}) + i = 0 \tag{8}$$

for the algebraic variable ϕ_2

$$\phi_{\mathbf{2}} = -\left(\kappa\hat{\mathbf{D}}_{\phi_2} + \sigma\hat{\mathbf{D}}_{\phi_1}\right)^{-1}\left[\sigma\hat{\mathbf{D}}_{\phi_1}(\phi_{\mathbf{1}} - \phi_{\mathbf{2}})\right. \tag{9}$$

$$\left.\kappa\left(\frac{t_+ - t_-}{f}\right)\hat{\mathbf{D}}_{\ln c}\ln(\mathbf{c}) + i\right]. \tag{10}$$

A unique solution of (9) exists if one of the potentials is set as a reference. Since only the potential difference, rather than the actual potential values, is important, this reference can be used. If no reference is set, then the range of potentials that would give the same potential difference would be infinite and there would be an infinite number of solutions to (9). Reformulating (4) using (9) gives the following equation system

$$\begin{bmatrix} M_{11} & M_{12} \\ 0 & M_{22} \end{bmatrix} \begin{bmatrix} \dot{\mathbf{c}} \\ \dot{\phi}_{\mathbf{1}} - \dot{\phi}_{\mathbf{2}} \end{bmatrix} = \begin{bmatrix} \hat{A}_{11} & 0 \\ 0 & \hat{A}_{22} \end{bmatrix} \begin{bmatrix} \mathbf{c} \\ \phi_{\mathbf{1}} - \phi_{\mathbf{2}} \end{bmatrix} \tag{11a}$$

$$+ \begin{bmatrix} 0 \\ B_1 \end{bmatrix} \ln(\mathbf{c}) + \begin{bmatrix} 0 \\ B_2 \end{bmatrix} i \tag{11b}$$

$$y = \begin{bmatrix} 0 & \tilde{C} \end{bmatrix} \begin{bmatrix} \mathbf{c} \\ \phi_{\mathbf{1}} - \phi_{\mathbf{2}} \end{bmatrix} + \tilde{D}_1 \ln(\mathbf{c}) + \tilde{D}_2 i \tag{11c}$$

whose trajectories evolve along the manifold defined by (7). The general form of (11) is

$$M\dot{x} = Ax + \tilde{B}_1 \ln(c) + \tilde{B}_2 i \tag{12a}$$

$$y = Cx + \tilde{D}_1 \ln(c) + \tilde{D}_2 i \tag{12b}$$

with state $x := [\mathbf{c}^T,\ \phi_{\mathbf{1}}{}^T - \phi_{\mathbf{2}}{}^T]^T$ where $c \in \mathbb{R}_+^n$ and $\phi_1 - \phi_2 \in \mathbb{R}^n$. By inverting the "mass" matrix M, (11a) can be written as a standard dynamic system

$$\dot{x} = A_m x + B_{1,m} \ln(c) + B_{2,m} i. \tag{13}$$

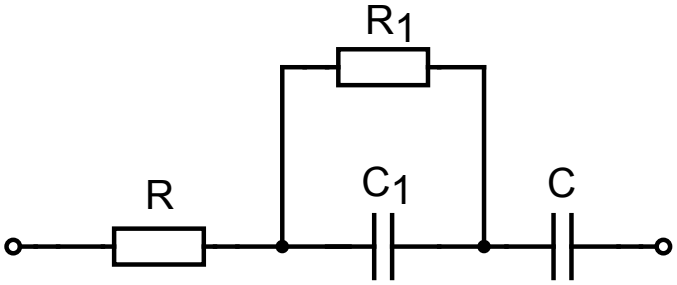

Figure 2: Classical circuit.

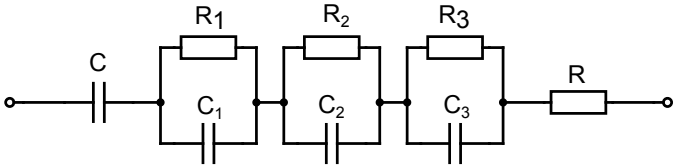

Figure 3: Dynamic circuit.

III. Equivalent Circuit Models

Several circuits to be synthesized from the PB model (13) will now be introduced. In the literature, a number of equivalent circuit models can be found, so to make the circuit synthesis problem tractable, the class of circuits which will be considered is restricted to the *classical*, *ladder* and *dynamic* circuits which have seen widespread application and are compared in [9].

The classical model with added series capacitance term, shown in Fig. 2, is the simplest model and has dynamics

$$\begin{bmatrix}\dot{x}_1\\ \dot{x}_2\end{bmatrix} = \begin{bmatrix}0 & 0\\ 0 & -\frac{1}{R_1C_1}\end{bmatrix}\begin{bmatrix}x_1\\ x_2\end{bmatrix} + \begin{bmatrix}\frac{1}{C}\\ \frac{1}{C_1}\end{bmatrix} i \tag{14a}$$

$$V = x_1 + x_2 + Ri. \tag{14b}$$

Incorporating additional time constants to this circuit by the inclusion of more RC branches results in the dynamic circuit, shown in Fig. 3, with dynamics

$$\begin{bmatrix}\dot{x}_1\\ \dot{x}_2\\ \dot{x}_3\\ \dot{x}_4\end{bmatrix} = \begin{bmatrix}0 & 0 & 0 & 0\\ 0 & -\frac{1}{R_1C_1} & 0 & 0\\ 0 & 0 & -\frac{1}{R_2C_2} & 0\\ 0 & 0 & 0 & -\frac{1}{R_3C_3}\end{bmatrix}\begin{bmatrix}x_1\\ x_2\\ x_3\\ x_4\end{bmatrix} + \begin{bmatrix}\frac{1}{C}\\ \frac{1}{C_1}\\ \frac{1}{C_2}\\ \frac{1}{C_3}\end{bmatrix} i \tag{15a}$$

$$V = x_1 + x_2 + x_3 + x_4 + R_s i. \tag{15b}$$

The third circuit which will be studied is the ladder circuit

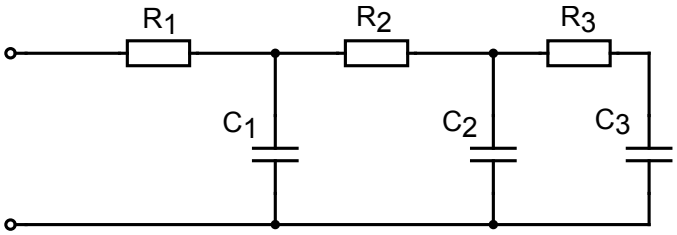

Figure 4: Ladder circuit.

of Fig. 4

$$\begin{bmatrix}\dot{x}_1\\ \dot{x}_2\\ \dot{x}_3\end{bmatrix} = \begin{bmatrix}-\frac{1}{R_2C_1} & \frac{1}{R_2C_1} & 0\\ \frac{1}{R_2C_2} & -\frac{R_2+R_3}{R_3R_2C_2} & \frac{1}{R_3C_2}\\ 0 & \frac{1}{R_3C_3} & -\frac{1}{R_3C_3}\end{bmatrix}\begin{bmatrix}x_1\\ x_2\\ x_3\end{bmatrix} + \begin{bmatrix}\frac{1}{C_1}\\ 0\\ 0\end{bmatrix} i \tag{16a}$$

$$V = x_1 + R_1 i. \tag{16b}$$

IV. Circuit Synthesis

In order to synthesize the three circuits (14), (15) and (16), the nonlinear PB model (13) is linearised around the equilibrium concentration c_e, where the concentration has diffused to a flat distribution, resulting in the following dynamics

$$\dot{x} = \big(A_m + [B_{1,m}/c_e\ 0]\big)x + B_{2,m} i \tag{17a}$$

$$y = \big(C + [\tilde{D}_1/c_e\ 0]\big)x + \tilde{D}_2 i. \tag{17b}$$

The logarithmic nonlinearity of (13) is relatively benign when $c_e \gg 0$ and only becomes significant when the concentration approaches zero. The near linear voltage-current dynamics of supercapacitors makes them more suitable for circuit realisation than other electrochemical devices such as lithium ion batteries, which exhibit highly nonlinear behaviour, due to the Butler-Volmer equation and OCV curve [18].

The dimensionality n of the discretised physical state-space system (17) is, in general, greater than the number of RC branches of typical equivalent circuit models, which most commonly have 2 or 3 branches [9]. In order for the boundary conditions to be implemented in (17), it was found that the electrode domain required a minimum of three discretisation elements and the separator required a minimum of two elements. This meant that the minimum dimensionality for the PB model in (17) was nine and, for circuit synthesis, the order of (17) needed to be reduced. There are a number of methods for model order reduction [28] with the balanced truncation method being implemented in this work [20]. The first stage of this method is to introduce the observability operator $\Psi_o : \mathbb{R}^n \to \mathcal{L}_2^e[0, t_1]$ where

$$\|y\|_2^2 = \langle x_0^* \Psi_o^*, \Psi_o x_0 \rangle \tag{18}$$

such that the observability grammian Y_o can be defined by

$$Y_o = \Psi_o^* \Psi_o = \int_0^{t_1} e^{A^*\tau} C^* C e^{A\tau} d\tau. \tag{19}$$

This self-adjoint operator maps the initial conditions to the outputs lying in the $\mathcal{L}_2^e$ Hilbert space. Similarly, the controllability operator $\Psi_c : \mathcal{L}_2^e[-t_2, 0] \to \mathbb{R}^n$

$$x_0 = \Psi_c u \tag{20}$$

defines the controllability grammian X_c

$$X_c = \Psi_c^* \Psi_c = \int_{-t_2}^{0} e^{A^*\tau} B^* B e^{A\tau} d\tau \tag{21}$$

which maps all inputs $u \in \mathcal{L}_2^e[-t_2, 0]$ to the initial condition $x_0 \in \mathbb{R}^n$. If a linear system is Hurwitz stable, controllable and observable, with system matrices (A, B, C, D), then it has a balanced realisation meaning that there exists a transformation matrix T such that the equivalent system $(\tilde{A}, \tilde{B}, \tilde{C}, \tilde{D}) = (T\tilde{A}T^{-1}, T\tilde{B}, \tilde{C}T^{-1}, D)$ satisfies

$$\tilde{X}_c = \tilde{Y}_o = \Sigma \tag{22}$$

with diagonal $\Sigma > 0$. The states that are least controllable in this equivalent system are also least observable. The error between a balanced system G and a reduced order system G_r is bounded by

$$\|G - G_r\|_\infty \geq \sigma_{r+1} \tag{23}$$

where $\sigma_1 \geq \sigma_2 \geq \cdots \geq \sigma_r \geq \sigma_{r+1} \geq \cdots \geq \sigma_n$ are the singular values of the Hankel operator $\Gamma_G = \Psi_o \Psi_c : \mathcal{L}_2^e[-t_2, 0] \rightarrow \mathcal{L}_2^e[0, t_1]$ which maps the model input to the output [20]. In this truncation method, the (balanced) state-space matrices are partitioned by

$$A = \begin{bmatrix} A_{11} & A_{12} \\ A_{21} & A_{22} \end{bmatrix} \quad B = \begin{bmatrix} B_1 \\ B_2 \end{bmatrix} \quad C = \begin{bmatrix} C_1 & C_2 \end{bmatrix} \tag{24}$$

and the resulting reduced order model (A_{11}, B_1, C_1, D) has frequency domain form

$$G_r(s) = C_1(Is - A_{11})^{-1}B_1 + D \tag{25}$$

which is balanced with Hankel singular values $\sigma_1 \ldots \sigma_r$ [20]. Reducing the order of the system in this manner means that the error of the input/output response of the reduced order model depends on the model order and can be lower bounded by σ_{r+1}.

The requirement that the system matrix A be Hurwitz for the balanced truncation method is violated by (17a) since n_i of the dynamic modes of this system are integrators. This problem was overcome by removing the integrators from the system, performing the model order reduction on the remaining Hurwitz subsystem and then combining this reduced order system back with the integrators. This means that the size of the reduced order system can never be less than n_i+1. However, in synthesis, the n_i integrator states combine to form a single lumped capacitor. This is shown by considering the dynamics of the integrator states $x_i \in \mathbb{R}^{n_i}$

$$\dot{x}_i = B_{int} i \tag{26a}$$

$$y_i = C_{int} x_i \tag{26b}$$

where $B_{int} \in \mathbb{R}^{n_i \times 1}, C_{int} \in \mathbb{R}^{1 \times n_i}$ such that the integrator capacitance $\mathfrak{C}$ is given by

$$\mathfrak{C} = C_{int} B_{int}. \tag{27}$$

For this reason, the controllability and observability operators are defined to operate on the $\mathcal{L}_2^e$ space, not the full $\mathcal{L}_2$ space. By defining the temporal domain to be a closed set $[-t_2, t_1]$ instead of the open set $(-\infty, \infty)$ as is used with the $\mathcal{L}_2$ space, then the dynamics of (17a) remain bounded for bounded inputs in finite time [29].

Parameter	Value	Units
Global Parameters		
$\frac{dq_+}{dq} = \frac{dq_-}{dq}$	-0.5	
t_+	0.55	
T	298	K
Electrode Domain		
κ	0.0195	S m^{-1}
D	2.09 $\times 10^{-12}$	m^2 s^{-1}
ϵ	0.67	
σ	0.0521	S m^{-1}
aC	42 $\times 10^6$	F m^{-2}
α	42 $\times 10^6$	F m^{-2}
β	10 $\times 10^6$	F m^{-2}
Separator Domain		
κ	0.0312	S m^{-1}
D	3.34 $\times 10^{-12}$	m^2 s^{-1}
ϵ	0.6	

Table I: Parameters for the PB supercapacitor model [10].

In addition to the Hurwitz condition, the system is also required to be both observable and controllable for a balanced realisation. These properties were studied in [30], where it was found that the nonlinear model was fully controllable but lost observability when the two transference numbers, t_+ and t_- in (1b), were equal. The presence of unobservable states with equal transference numbers occurs because there is no induced potential gradient caused by an imbalance of positive and negative electrolyte ions. This means that no knowledge about the concentrations could be gained from measurements of the voltage. However, for unequal transference numbers, which occurs in most supercapacitor electrolytes [31], the model was shown to be fully observable.

The transfer function $G(s)$ of the reduced order system (17) is known as the impedance function, giving the s-domain gain from current to voltage. When (17) was reduced to a three state system using the parameters from Table I the impedance function was

$$G(s) = \frac{V(s)}{I(s)} = \frac{(s + 6.56)(s + 1.59)(s + 0.29)}{s(s + 5.62)(s + 1.4)}. \tag{28}$$

Equivalent circuit realisations of the impedance function (28) will now be obtained using passive network synthesis. Passive network synthesis was studied extensively in the electrical engineering community in the 1930s [32, 33] with the goal being to understand and simulate complex dynamical systems using electrical components [34]. Interest in this field died down in the 1960s even though many problems still remained open. Network synthesis has recently witnessed a revival due to the application of modern mathematical tools to the classical methods [35] and its application to mechanical systems through the discovery of the inerter [36].

The key requirement for circuit synthesis of an impedance function is that $G(s)$ must be a positive real function. Positive real functions satisfy:

1) $G(s)$ is real for real s.

2) Real $G(s) \geq 0$ for real $s \geq 0$.

Positive realness is equivalent to showing that the system is passive, i.e. non energy generating [37]. Passivity of the supercapacitor model has been shown for both the nonlinear discretised system and for the fundamental nonlinear partial differential algebraic equations [38]. This implies that the PDE model could be realised by a RC circuit of infinite dimension, but, this is beyond the scope of this paper.

The positive-real conditions are satisfied by (28). Realising a transfer function in terms of a circuit is equivalent to realising it in terms of a state-space system that has a particular structure. State transformation operations imply that transfer functions have a non-unique state-space representation and this explains the vast array of circuit models that can be found in the literature. By restricting the class of circuits to the classical, dynamic and ladder circuits of [9], circuit realisations can be obtained, although it is pointed out that there exists a much wider class of circuits that could be realised by the proposed approach, but are not considered in this paper.

The methodology of network synthesis is to expand the positive real impedance function $G(s)$ around some point, such as a pole at $s = 0$. The various components of this expansion can then be realised by passive electrical components such as resistors, capacitors and inductors [39]. The realisation of the impedance function (28) in terms of the dynamic circuit (15) is known as the Foster form of the first kind [39] and is obtained by continuously removing a pole of $G(s)$ at $s = 0$. This is similar to performing a partial fraction expansion

$$G(s) = \frac{1}{k_0} + \frac{k_1}{s+\sigma_1} + \cdots + \frac{k_i}{s+\sigma_i} + \cdots + k_\infty. \tag{29}$$

The resistances and capacitances of the circuit can then be obtained by the following rules

$$C = \frac{1}{k_0} \quad C_i = \frac{1}{k_i} \quad R_i = \frac{k_i}{\sigma_i} \quad R = k_\infty. \tag{30}$$

By reducing the order of the reduced system to one, the classical circuit of (14) is realised. An alternative method for obtaining the RC components for the dynamic circuit would be to take the eigen-decomposition of the reduced order physical system (17) and then match up the system matrix coefficients to that of (15), since both would have diagonal structures.

The ladder circuit (16) can be realised from the impedance function by the continuous removal of poles at $s = \infty$. This representation is known as the Cauer form of the first kind [39] and can be obtained by taking a continuous fraction expansion of the impedance function

$$G(s) = \alpha_1 + \cfrac{1}{\alpha_2 s + \cfrac{1}{\alpha_3 + \cfrac{1}{\alpha_4 s + \cfrac{1}{\alpha_5 + \ddots \; \alpha_{r-1} + \frac{1}{\alpha_r s}}}}}. \tag{31}$$

The resistors and capacitors of the circuit can then be obtained with

$$R_i = \alpha_{2i-1} \quad C_i = \alpha_{2i} \quad \text{for } i = 1, \ldots, r/2. \tag{32}$$

The Cauer form of the second kind [39] of (28) has the resistors and capacitors swapped around in Fig. 4. The values of the resistors and capacitors for the three circuits obtained by the synthesis procedure are given in Table II for the SAFT America supercapacitor described by the parameters from Table I. It is noted that the proposed synthesis method allows a wide class of circuits to be synthesized, with this class not being restricted to the three circuits described. The Bode plots for the three circuits match the full order linearised PB model as shown in Fig 5. This is to be expected since the circuits are simply reduced order realisations of the physical impedance function.

Component	Classical	Dynamic	Ladder
R_1	$6.2 \times 10^{-4}\ \Omega$	$3.75 \times 10^{-4}\ \Omega$	$2.5 \times 10^{-3}\ \Omega$
R_2		$3.15 \times 10^{-4}\ \Omega$	$9.8 \times 10^{-4}\ \Omega$
R_3		$2.52 \times 10^{-4}\ \Omega$	$4 \times 10^{-3}\ \Omega$
R	$2.52 \times 10^{-3}\ \Omega$	$2.52 \times 10^{-3}\ \Omega$	
C_1	$431\ F$	$475\ F$	$285.9\ F$
C_2		$2.26 \times 10^{3}\ F$	$549.6\ F$
C_3		$1.3 \times 10^{6}\ F$	$249.6 \times 10^{-6}\ F$
C	$1.05 \times 10^{3}\ F$	$1.05 \times 10^{3}\ F$	

Table II: Resistor and capacitor values for the synthesized classical, dynamic and ladder circuits.

Using this approach, quantitative estimates for the the errors introduced at each step of the synthesis process (discretisation, linearisation and model order reduction) can be obtained when the full order PB model is treated as describing the true dynamics of the system. This contrasts with the rather qualitative errors discussed with fitted EC circuits. The singular values of the Hankel norm describe the error bound for the reduced order system and are shown for a 20 state discretisation of (17) in Fig. 6. The first three singular values in this plot have been removed since they relate to the integrator states. For this discretisation, 12 states were related to the concentration c with the remaining eight being related to the potential difference $\phi_1 - \phi_2$. This shows that the concentration states have a greater impact on the input/output dynamics of (17) than the potential states. This is because the concentration states evolve by a diffusion process, which

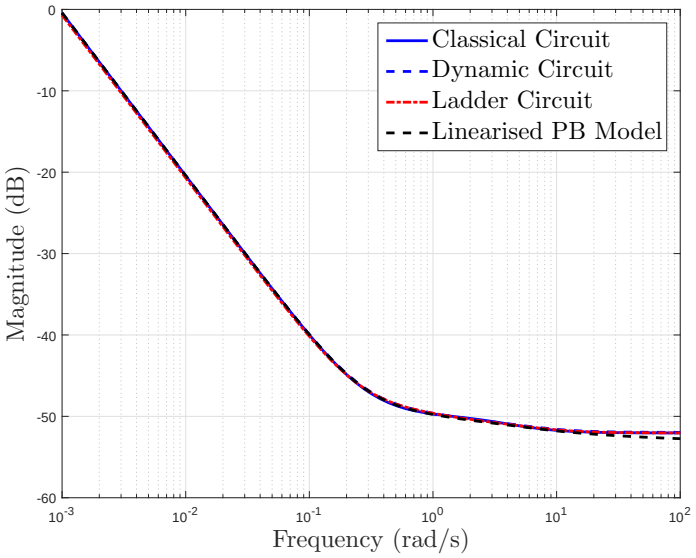

(a) Magnitude of $G(s)$.

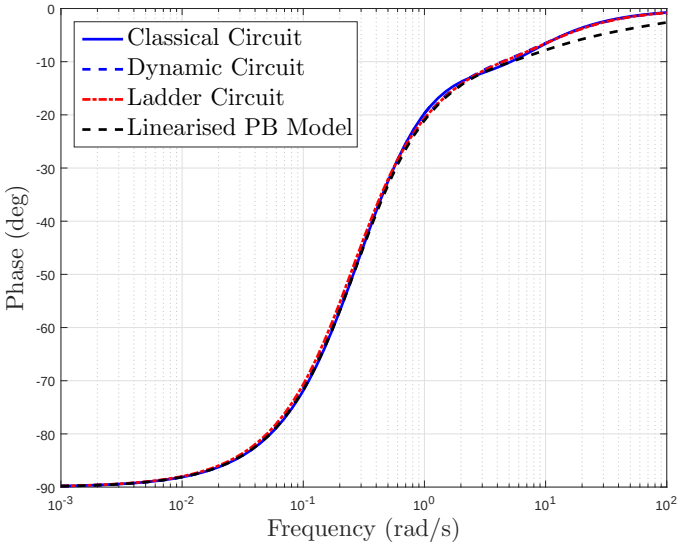

(b) Phase of $G(s)$.

Figure 5: Bode plot of the three synthesized circuits and full order linearised physical model.

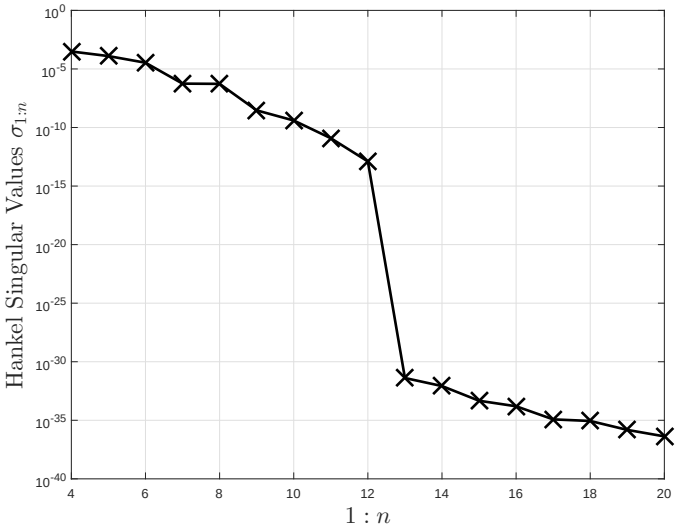

Figure 6: Singular values of the Hankel operator Γ_G.

is much slower than the rapidly decaying, fast dynamics associated with the potentials. This suggests that there is no advantage gained in increasing the number of RC branches beyond the number of concentration states $n_c - n_i$ when this synthesis process is used.

Recently, circuits have been developed for specific charging conditions such as charge relaxation [40]. With the proposed PB approach, there should be a much broader range of dynamics that are considered in forming the impedance functions. This should result in more generalised synthesized circuits that are designed for a broader range of charging conditions. The ability to realise the physical dynamics in terms of both the ladder and the dynamic circuits contrasts with the view in the literature which gives each of these circuits a distinct physical interpretation; the ladder circuit is said to describe ion movement within a pore while the dynamic circuit is said to model double layer effects [9]. The analysis of this paper suggests that the physical interpretation of these circuits is not as well defined as that, with each of the modelled phenomenon contributing to the components of each branch. The admittance function $F(s)$, which is the inverse of the impedance function $G(s)$, can also be synthesized in terms of resistors and inductors [39]. The PB model is transformed into a circuit and it is believed that this transformation can not occur in the opposite direction, i.e. going from the circuit equations to the model PDEs. However, it is pointed out that developing PB models by considering the physics would be a better approach than reverse synthesizing circuits.

The proposed circuit synthesis method is flexible since it can be applied to general PB models describing additional physical phenomena. For example, including the linear dependence of electrolyte conductivity with concentration

$$\kappa = \kappa_0 c, \tag{33}$$

which is often neglected due to the assumptions of dilute solution thoery [10], changes the state-space system to

$$\begin{bmatrix} \epsilon & \frac{aC}{F}(t_- \frac{dq_+}{dq} + t_+ \frac{dq_-}{dq}) & 0 \\ 0 & aC & 0 \\ 0 & 0 & 0 \end{bmatrix} \begin{bmatrix} \dot{c} \\ \dot{\phi}_1 - \dot{\phi}_2 \\ \dot{\phi}_2 \end{bmatrix} = \begin{bmatrix} 0 \\ 0 \\ 1 \end{bmatrix} i$$
$$+ \begin{bmatrix} D\frac{\partial^2}{\partial \chi^2} & 0 & 0 \\ 0 & \sigma \frac{\partial^2}{\partial \chi^2} & \sigma \frac{\partial^2}{\partial \chi^2} \\ \frac{\kappa_0 RT(t_+ - t_-)}{F} \frac{\partial}{\partial \chi} & \sigma \frac{\partial}{\partial \chi} & \kappa_0 c \frac{\partial}{\partial \chi} + \sigma \frac{\partial}{\partial \chi} \end{bmatrix} \begin{bmatrix} c \\ \phi_1 - \phi_2 \\ \phi_2 \end{bmatrix} \tag{34}$$

whose linearised impedance is

$$G(s) = \frac{V(s)}{I(s)} = \tag{35}$$
$$\frac{(s+4.76)(s+0.3)(s+2.95\times10^{-5})(s+3.27\times10^{-5})}{s(s+3.74)(s+2.9\times10^{-5})(s+3.27\times10^{-6})}. \tag{36}$$

As well as electrolyte conductivity, the capacitance aC has also been shown to vary during charging. Several models have been proposed to account for this relationship, with the most popular being the Guoy-Chapman-Stern model [1]. In the region of low voltage, this relationship can be approximated by a linear fit

$$aC = \alpha + \beta(\phi_1 - \phi_2). \tag{37}$$

This relationship changes the state-space system to

$$\begin{bmatrix} \epsilon & \frac{\alpha+\beta(\phi_1-\phi_2)}{F}(t_-\frac{dq_+}{dq} + t_+\frac{dq_-}{dq}) & 0 \\ 0 & \alpha+\beta(\phi_1-\phi_2) & 0 \\ 0 & 0 & 0 \end{bmatrix} \begin{bmatrix} \dot{c} \\ \dot{\phi}_1 - \dot{\phi}_2 \\ \dot{\phi}_2 \end{bmatrix} = + \begin{bmatrix} D\frac{\partial^2}{\partial\chi^2} & 0 & 0 \\ 0 & \sigma\frac{\partial^2}{\partial\chi^2} & \sigma\frac{\partial^2}{\partial\chi^2} \\ 0 & \sigma\frac{\partial}{\partial\chi} & \kappa\frac{\partial}{\partial\chi} + \sigma\frac{\partial}{\partial\chi} \end{bmatrix} \begin{bmatrix} c \\ \phi_1 - \phi_2 \\ \phi_2 \end{bmatrix} + \begin{bmatrix} 0 \\ 0 \\ \kappa\left(\frac{RT(t_+-t_-)}{F}\right)\frac{\partial}{\partial\chi} \end{bmatrix} \ln(c) + \begin{bmatrix} 0 \\ 0 \\ 1 \end{bmatrix} i. \tag{38}$$

and the impedance for a given α and β in Table I to

$$G(s) = \frac{V(s)}{I(s)} = \frac{(s+6.04)(s+1.46)(s+0.27)(s+0.0031)}{s(s+5.17)(s+1.29)(s+0.003)}. \tag{39}$$

Both impedance functions (35) & (39) are positive real functions and so can be synthesized by passive circuit elements. The method can also be easily updated to generate local circuits applicable to any operating region besides the equilibrium concentration by changing the linearisation point of the model.

As discussed in the introduction, circuits approximate the local dynamics of a nonlinear supercapacitor model in a given operating region. During a charging profile, the state of the supercapacitor may leave this region, necessitating the need for a new circuit to be generated, typically using parameter estimation methods [41]. This parameter estimation problem for the circuit components can be re-cast as a synthesis problem of the PB model. Fig. 7 shows the percentage deviation from their original values of the three time constants of the dynamic circuit (15) that were synthesized from (1) using an input current of $i = 10 + 10\sin(0.1t)$ A m^{-2}. Unlike Fig. 5, Fig. 7 does not describe the accuracy of the circuit realisation, but instead analyses how the components of the dynamic circuit realisation would vary during a charge to account for the nonlinearity of the PB model. The three RC branches shown in Fig. 7 relate to different time constants with $C_1R_1 < C_2R_2 < C_3R_3$. It was found that only the time constant C_3R_3, which is related to long term dynamics, changed significantly during this charging profile. This is because the localised component of the PB model dynamics that changes during the charging profile is due to the $\ln(c)$ nonlinearity, which is solely a function of the concentration. Since the concentration exhibits slow diffusion dynamics via (1b), only the long term time constants

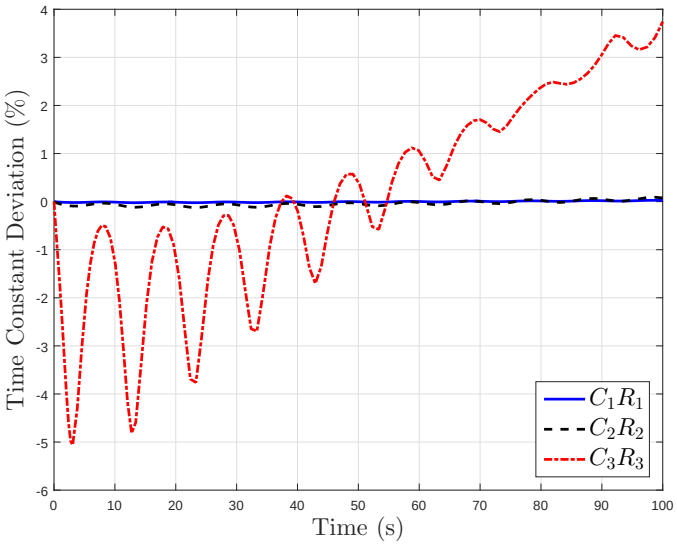

Figure 7: Variation of the time constants of the dynamic circuit during a charge with sinusoidal current.

are local. If the electrochemical equations were linear, then the circuit component values would be fixed. However, the circuit component values would still be dependent upon the parameters of the PB model, such as temperature and porosity factor, as these parameters affect the impedance function. The proposed method can easily accommodate for this dependency. Since no analytic expression was obtained for the circuit components in terms of the physical parameters, the synthesis process was carried out at each time step of the simulation. Although, since the numerical procedure for the synthesis was fairly efficient, this process was not computational exhaustive. The trajectory based synthesis method proposed here should be more accurate than circuits synthesized around an equilibrium point.

V. Conclusion

In this paper, a method for synthesising electrical circuits from physical supercapacitor models has been proposed. This method used model discretisation, linearisation, balanced model order reduction and passive network synthesis. The method is flexible since a wide class of circuits can be realised from a wide class of physical models. The circuits were validated by comparing their frequency responses to that of a linearised physical model. The aim of this paper is to give a greater understanding to the physical interpretation of equivalent circuit models and also to enable the synthesis of more general circuits whose impedance function would be generated by considering the device physics, not by experimental fitting.

Acknowledgments

Support from the UK Engineering and Physical Sciences Research Council is gratefully acknowledged.

References

[1] M. Lu, F. Beguin, and E. Frackowiak. *Supercapacitors: Materials, Systems and Applications*. John Wiley & Sons, 2013.

[2] X. Luo, J. Wang, M. Dooner, and J. Clarke. Overview of current development in electrical energy storage technologies and the application potential in power system operation. *Applied Energy*, 137:511–536, 2015.

[3] M. Winter and R. J. Brodd. What are batteries, fuel cells, and supercapacitors? *Chemical Reviews*, 104(10):4245–4270, 2004.

[4] F. Ongaro, S. Saggini, and P. Mattavelli. Li-ion battery-supercapacitor hybrid storage system for a long lifetime, photovoltaic-based wireless sensor network. *IEEE Transactions on Power Electronics*, 27(9):3944–3952, 2012.

[5] N. Devillers, S. Jemei, M. Péra, D. Bienaimé, and F. Gustin. Review of characterization methods for supercapacitor modelling. *Journal of Power Sources*, 246:596–608, 2014.

[6] F. Rafik, H. Gualous, R. Gallay, A. Crausaz, and A. Berthon. Frequency, thermal and voltage supercapacitor characterization and modeling. *Journal of Power Sources*, 165(2):928–934, 2007.

[7] R. L. Spyker and R. M. Nelms. Classical equivalent circuit parameters for a double-layer capacitor. *IEEE Transactions on Aerospace and Electronic Systems,*, 36(3):829–836, 2000.

[8] S. Buller, M. Thele, R. W. A. A. De Doncker, and E. Karden. Impedance-based simulation models of supercapacitors and li-ion batteries for power electronic applications. *IEEE Transactions on Industry Applications*, 41(3):742–747, 2005.

[9] L. Zhang, Z. Wang, X. Hu, F. Sun, and D. G. Dorrell. A comparative study of equivalent circuit models of ultracapacitors for electric vehicles. *Journal of Power Sources*, 274:899–906, 2015.

[10] M. W. Verbrugge and P. Liu. Microstructural analysis and mathematical modeling of electric double-layer supercapacitors. *Journal of The Electrochemical Society*, 152(5):D79–D87, 2005.

[11] S. Allu, B. Velamur Asokan, W. A. Shelton, B. Philip, and S. Pannala. A generalized multi-dimensional mathematical model for charging and discharging processes in a supercapacitor. *Journal of Power Sources*, 256(0):369 – 382, 2014.

[12] R. Drummond, D. A. Howey, and S. R. Duncan. Low-order mathematical modelling of electric double layer supercapacitors using spectral methods. *Journal of Power Sources*, 277:317–328, 2015.

[13] G. Madabattula and S. K. Gupta. Modeling of supercapacitor. In *Proc. of the 2012 COMSOL Conference*, Bangalore, India, 2012.

[14] A. Romero-Becerril and L. Alvarez-Icaza. Reduced order dynamical model for supercapacitors. In *Proc. of the 7th IEEE International Conference on Electrical Engineering Computing Science and Automatic Control (CCE)*, pages 71–76, Tuxtla Gutierrez, Mexico, 2010.

[15] A. d'Entremont and L. Pilon. First-principles thermal modeling of electric double layer capacitors under constant-current cycling. *Journal of Power Sources*, 246:887–898, 2014.

[16] V. Srinivasan and J. W. Weidner. Mathematical modeling of electrochemical capacitors. *Journal of the Electrochemical Society*, 146(5):1650–1658, 1999.

[17] M. Doyle, T. F. Fuller, and J. Newman. Modeling of galvanostatic charge and discharge of the lithium/polymer/insertion cell. *Journal of the Electrochemical Society*, 140(6):1526–1533, 1993.

[18] A. Bizeray, S. Duncan, and D. A. Howey. Advanced battery management systems using fast electrochemical modelling. In *Proc. of the 4th IET Hybrid and Electric Vehicles Conference (HEVC)*, London, UK, 2013.

[19] N. Chaturvedi, R. Klein, J. Christensen, J. Ahmed, and A. Kojic. Algorithms for advanced battery-management systems. *Control Systems, IEEE*, 30(3):49–68, 2010.

[20] G. Dullerud and F. Paganini. *Course in Robust Control Theory*. Springer-Verlag New York, 2000.

[21] E. A. Guillemin. *Synthesis of Passive Networks: Theory and Methods Appropriate to the Realization and Approximation Problems*. Wiley New York:, 1957.

[22] K. A Smith, C. D. Rahn, and C. Y. Wang. Control oriented 1D electrochemical model of lithium ion battery. *Energy Conversion and Management*, 48(9):2565–2578, 2007.

[23] M. Jun, K. Smith, and P. Graf. State-space representation of li-ion battery porous electrode impedance model with balanced model reduction. *Journal of Power Sources*, 273:1226–1236, 2015.

[24] S. Raël and M. Hinaje. Using electrical analogy to describe mass and charge transport in lithium-ion batteries. *Journal of Power Sources*, 222:112–122, 2013.

[25] R. Drummond, D. A. Howey, and S. R. Duncan. Parameter estimation of an electrochemical supercapacitor model. *Proc. of the European Control Conference*, Aarlberg, Denmark, 2016.

[26] B. Wu, M. A. Parkes, V. Yufit, L. De Benedetti, S. Veismann, C. Wirsching, F. Vesper, R. F. Martinez-Botas, A. J. Marquis, G. J. Offer, and N. P. Brandon. Design and testing of a 9.5 kwe proton exchange membrane fuel cell-supercapacitor passive hybrid system. *International Journal of Hydrogen Energy*, 39(15):7885 – 7896, 2014.

[27] L. N. Trefethen. *Spectral Methods in MATLAB*, volume 10. SIAM, Philadelphia, USA, 2000.

[28] A. C. Antoulas, D. C. Sorensen, and S. Gugercin. A survey of model reduction methods for large-scale systems. *Contemporary Mathematics*, 280:193–220, 2001.

[29] U. Jönsson. Lecture notes on integral quadratic constraints. *Department of Mathematics, KTH, Stock-*

holm, ISBN 1401-2294, 2000.

[30] R. Drummond and S. R. Duncan. On observer performance for an electrochemical supercapacitor model for applications such as fault ride through. *Proc. of the Multi-Conference on Systems and Control*, Sydney, Australia, 2015.

[31] M. Galiński, A. Lewandowski, and I. Stępniak. Ionic liquids as electrolytes. *Electrochimica Acta*, 51(26):5567–5580, 2006.

[32] R. Bott and R. J. Duffin. Impedance synthesis without use of transformers. *Journal of Applied Physics*, 20(8):816–816, 1949.

[33] O. Brune. *Synthesis of a finite two-terminal network whose driving-point impedance is a prescribed function of frequency*. PhD thesis, Massachusetts Institute of Technology, 1931.

[34] P. D. Cha, J. J. Rosenberg, and C. L. Dym. *Fundamentals of Modeling and Analyzing Engineering Systems*. Cambridge University Press, Cambridge, UK, 2000.

[35] M. Z. Q. Chen and M. C. Smith. *Electrical and Mechanical Passive Network Synthesis*, pages 35–50. Springer London, London, 2008.

[36] M. C. Smith. Synthesis of mechanical networks: The inerter. *IEEE Transactions on Automatic Control*, 47(10):1648–1662, 2002.

[37] J. C. Willems. Dissipative dynamical systems part i: General theory. *Archive for Rational Mechanics and Analysis*, 45(5):321–351, 1972.

[38] R. Drummond and S. R. Duncan. A Lyapunov function for a PDE model of a supercapacitor. *Proc. of the Control and Decision Conference*, Osaka, Japan, 2015.

[39] C. L. Wadhwa. *Network Analysis & Synthesis (Including Linear System Analysis)*. New Age International, New Delhi, India, 2007.

[40] D. Torregrossa, M. Bahramipanah, E. Namor, R. Cherkaoui, and M. Paolone. Improvement of dynamic modeling of supercapacitor by residual charge effect estimation. *IEEE Transactions on Industrial Electronics,*, 61(3):1345–1354, 2014.

[41] L. Zhang, Z. F. Wang, and G. Dorrell. Online parameter identification of ultracapacitor models using the extended Kalman filter. *Energies*, 7(5):3204–3217, 2014.